Global Biogeochemical Cycles

RESEARCH ARTICLE
10.1029/2023GB007721

The Role of Glacier Erosion in Riverine Particulate Organic Carbon Export

Megan I. Behnke[1], Jason B. Fellman[1], Sonia Nagorski[1], Robert G. M. Spencer[2], and Eran Hood[1]

[1]Alaska Coastal Rainforest Center and Department of Natural Sciences, University of Alaska Southeast, Juneau, AK, USA, [2]Department of Earth, Ocean, and Atmospheric Science, Florida State University, Tallahassee, FL, USA

Key Points:

- Carbon isotope data show a petrogenic source contributed to glacier river particulate organic carbon (POC) entering Southeast Alaska fjords
- Glacier erosion and melt increased the river petrogenic POC:biospheric POC ratio, while non-glacial runoff lowered the ratio
- Heavily glacierized rivers can have high biospheric POC and sediment concentrations, implying high carbon burial potential in fjord sediments

Supporting Information:

Supporting Information may be found in the online version of this article.

Correspondence to:

M. I. Behnke,
mibehnke@alaska.edu

Citation:

Behnke, M. I., Fellman, J. B., Nagorski, S., Spencer, R. G. M., & Hood, E. (2023). The role of glacier erosion in riverine particulate organic carbon export. *Global Biogeochemical Cycles*, *37*, e2023GB007721. https://doi.org/10.1029/2023GB007721

Received 1 FEB 2023
Accepted 2 OCT 2023

Abstract Biospheric particulate organic carbon (POC_{bio}) burial and rock petrogenic particulate organic carbon (POC_{petro}) oxidation are opposing long-term controls on the global carbon cycle, sequestering and releasing carbon, respectively. Here, we examine how watershed glacierization impacts the POC source by assessing the concentration and isotopic composition ($\delta^{13}C$ and $\Delta^{14}C$) of POC exported from four watersheds with 0%–49% glacier coverage across a melt season in Southeast Alaska. We used two mixing models (age-weight percent and dual carbon isotope) to calculate concentrations of POC_{bio} and POC_{petro} within the bulk POC pool. The fraction POC_{petro} contribution was highest in the heavily glacierized watershed (age-weight percent: 0.39 ± 0.05; dual isotope: 0.42 (0.37–0.47)), demonstrating a glacial source of POC_{petro} to fjords. POC_{petro} was mobilized via glacier melt and subglacial flow, while POC_{bio} was largely flushed from the non-glacierized landscape by rain. Flow normalized POC_{bio} concentrations exceeded POC_{petro} concentrations for all streams, but surprisingly were highest in the heavily glacierized watershed (mean: 0.70 mgL^{-1}; range 0.16–1.41 mgL^{-1}), suggesting that glacier rivers can contribute substantial POC_{bio} to coastal waters. Further, the most heavily glacierized watershed had the highest sediment concentration (207 mgL^{-1}; 7–708 mgL^{-1}), and thus may facilitate long-term POC_{bio} protection via sediment burial in glacier-dominated fjords. Our results suggest that continuing glacial retreat will decrease POC concentrations and increase POC_{bio}:POC_{petro} exported from currently glacierized watersheds. Glacier retreat may thus decrease carbon storage in marine sediments and provide a positive feedback mechanism to climate change that is sensitive to future changes in POC_{petro} oxidation.

Plain Language Summary Particulate organic carbon (POC) in rivers can come from bedrock and the biosphere. When POC produced by vegetation and soils gets buried in fjords, it can be stored for hundreds of thousands of years. In contrast, when bedrock erodes and rock organic carbon reacts with oxygen, carbon previously stored long term can enter the atmosphere as carbon dioxide. Thus, understanding the balance between these two sources of POC and their fates can help predict future carbon cycling. Here, we study POC in glacial rivers, where bedrock erosion produces rock derived POC and where soil and forests produce biospheric POC. We show how much POC comes from each source across the glacial melt season in four rivers in Southeast Alaska whose watershed range in percent glacier coverage from 0% to 49%. The watershed with the largest glacier coverage produces the most rock-derived POC, providing evidence of the glacial source of rock-derived carbon that can occur in Southeast Alaskan fjords. However, the most glacial watershed also carries the highest concentration of POC from the biosphere and the most sediment, suggesting that glacier rivers play an outsized role in carrying both rock- and plant-derived carbon to fjords where its burial can help mitigate climate change.

1. Introduction

The amount of carbon stored in the atmosphere is small in comparison to the amount stored in the terrestrial biosphere, rocks, or the ocean (Hedges, 1992; Smith et al., 1993). The atmosphere is therefore sensitive to relatively small perturbations of carbon fluxes within and between these larger reservoirs. Rivers currently transport ~450 Tg yr^{-1} of organic carbon from continents to the ocean, more than half of which is in the particulate form (Kirschbaum et al., 2019). Modern particulate organic carbon derived from the biosphere (POC_{bio}) is a long-term carbon sink when it is buried in continental shelf sediments. Conversely, petrogenic (rock-derived) POC (POC_{petro}) that is oxidized during glacial erosion or export is a source of carbon dioxide (CO_2) to the atmosphere (Blattmann, 2022; Hedges, 1992; Hilton & West, 2020). The burial of POC_{bio} appears to respond more rapidly to

warming temperatures and increasing erosion than does the removal of atmospheric CO_2 via silicate weathering, suggesting that POC_{bio} burial will be the dominant atmospheric carbon sink during modern climate warming (Galy et al., 2015; Hilton, 2017). In this context, the source and fate of POC influence the storage and release of carbon over both shorter, human-relevant timeframes and geologic timescales (Berner, 1982; Hilton, 2017).

Globally, sediment fluxes from rivers to the ocean have shifted substantially due to anthropogenic impacts on sediment sources and transport pathways (Dethier et al., 2022). In the global north, the riverine sediment flux has decreased almost 50% in the past 40 years due to damming of rivers (Dethier et al., 2022). Undammed glacial rivers are an exception to this trend, with increases in glacial discharge associated with glacier volume loss projected to continue leading to higher sediment discharge into pro-glacial rivers in the coming decades (Bogen, 2008; Delaney & Adhikari, 2020). Riverine sediment fluxes into environments such as fjord systems that encourage deposition are a major pathway for POC burial and sequestration (Cui, Bianchi, Savage, & Smith, 2016; Galy et al., 2015). In turn, POC transport to the ocean is highest globally in small mountain rivers with steep terrain (Hilton, 2017; Hilton et al., 2008). High-latitude fjords thus have the potential to trap and sequester large amounts of POC_{petro} released from OC-bearing bedrock due to the high erosion rates brought on by glacier flow, especially in regions dominated by fast moving glaciers such as Southeast Alaska (Berg et al., 2021; Hallet et al., 1996; Herman et al., 2015; Smith et al., 2015). Rapid glacier retreat can temporarily increase export and fjord burial of POC_{petro} (Berg et al., 2021). However, extensive glacial retreat can increase the ratio of riverine POC_{bio} to POC_{petro}, due to vegetation expansion and the lower sediment and water yields from deglaciated landscapes (Buma & Barrett, 2015; Cui, Bianchi, Jaeger, & Smith, 2016; Hood et al., 2020; Milner et al., 2017; Walinsky et al., 2009). Steep, glacierized, high-latitude watersheds that deposit sediment and POC directly into deep fjords are ideal locations for terrestrial POC transfer and sediment deposition which facilitate organic carbon burial (of either petrogenic or biospheric origin). Thus, the relative balance of POC_{petro} and POC_{bio} transported from glacial rivers into fjords and the subsequent role of glacial rivers in land-to-ocean transport of OC needs to be further constrained.

This study quantifies the contribution of POC_{bio} and POC_{petro} to total POC concentrations in rivers draining four watersheds in coastal Southeast Alaska that span a glacierization gradient of 0%–49% and empty into the Lynn Canal fjord. To evaluate the petrogenic and biospheric contributions to riverine POC loads, we use (a) an age-weight percent OC relationship; and (b) an isotopic mixing model with $\delta^{13}C$ and $\Delta^{14}C$ isotopes that allow us to partition POC sources and calculate the concentrations of POC_{bio} and POC_{petro} across the six-month meltwater runoff season. We assess how watershed glacierization impacts POC_{petro} inputs to rivers and quantify the role of heavily glacierized watersheds in transporting modern POC_{bio} to coastal waters. These analyses provide new insights into how ongoing glacier retreat will impact the composition and fate of riverine POC delivered to fjords.

2. Methods

2.1. Watersheds Characteristics

The four study watersheds are adjacent to the Juneau Icefield (JIF) in the Coast Mountains of Southeast Alaska (Figure 1). Sampling occurred during the main runoff season (mid-April through October), a period that accounts for ~70%–90% of annual discharge from glacierized watersheds in the region (Hood et al., 2020). The JIF is rapidly thinning (Berthier et al., 2018) and is projected to decrease to a third of its current volume by 2100 (Ziemen et al., 2016). Three of the study watersheds, Herbert River, Cowee Creek, and Montana Creek, are glacierized and extend from sea level to the western edge of the JIF in the Alaska Coast Mountains. The Herbert River watershed (152 km^2) has the highest glacier coverage (49%) including a major outflow glacier from the JIF and includes a peatland-dominated tributary (Table 1). Small alpine glaciers (<10 km^2) cover 13% of Cowee Creek (Ch'eet' Taayí) watershed (110 km^2), while Montana Creek (Kaxdigoowu Héen) watershed (37 km^2) contains semi-permanent snow fields on recently deglaciated steep terrain and residual glacier ice (~2% coverage). The fourth watershed, unglacierized Peterson Creek (24 km^2), is a low relief, forested watershed with high wetland coverage that is representative of the coastal temperate rainforest landscape in the low elevation reaches of the glacierized watersheds. Herbert, Cowee, and Peterson drain directly into the Lynn Canal, the longest (140 km) and deepest fjord in North America, while Montana empties into the Mendenhall River less than 3 km from where it drains into the Lynn Canal. All four watersheds have anadromous Pacific salmon runs (*Oncorhynchus* spp.), which occur from July to October (Fellman et al., 2014).

A Cretaceous-Tertiary, erosion-resistant, foliated tonalite sill of the Coast Plutonic complex forms the tall peaks within the JIF and dominates the exposed areas of the Herbert, Cowee, and Montana bedrock geology

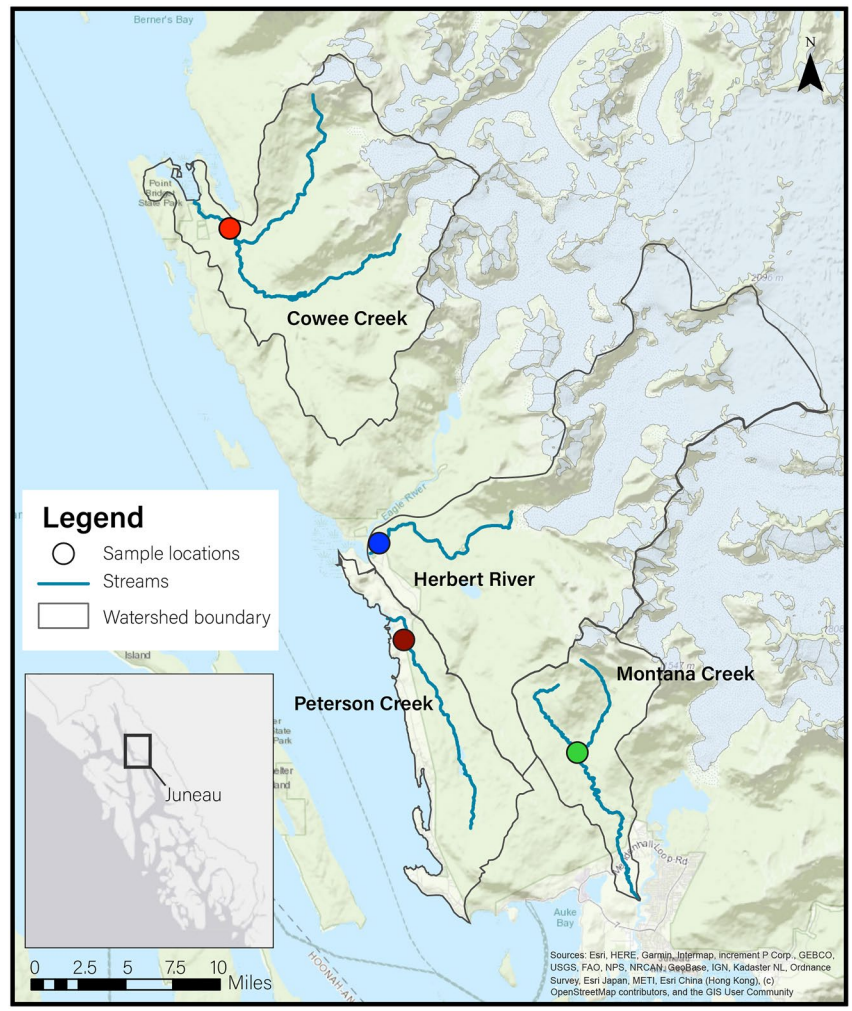

Figure 1. Map of study watersheds. Icefield and glacier extent is shown by gray hashing, and sampling locations are colored circles.

Table 1
Characteristics of the Study Watersheds

	Herbert River	Cowee Creek	Montana Creek	Peterson Creek
Watershed area (km^2)	152	110	37	24
Mean annual discharge (10^7 m^3)	65.3	36.3	8.9	4.5
Mean watershed elevation (m)	860	648	481	309
Mean watershed slope (deg)	18	23	21	12
Mean stream slope (deg)	9	10	11	6
Wetland coverage (%)	5	5	6	34
Glacier coverage (%)	49	13	2	0
Forest coverage (%)	25	57	66	92

Note. Discharge was measured at the sampling site (see Figure 1) for Herbert, Cowee, and Peterson, and measured ~5 km downstream from the Montana sampling location. Alpine, subalpine, and shrub ecosystems including bare rock and scree slopes account for the remaining watershed areas not reported by the percent coverage. Forested wetland ecosystems are considered as both forest and wetland coverage due to the presence of both sets of characteristics.

in the upper sections of those catchments where the glaciers occur (Wilson et al., 2015). Narrow lenses of POC_{petro}-bearing carbonaceous shale, phyllite, metalimestone, and metabasalt outcrop are minor portions within the tonalite-dominated areas of upper Herbert and Cowee, but the unexposed subglacial bedrock lithology can only be inferred as mostly tonalite (Wilson et al., 2015). Downstream of the tonalite and glaciers, the Herbert, Cowee, and Montana watersheds intersect the Taku accreted terranes that feature Permian-Cretaceous metamorphic rocks with sedimentary and volcanic protoliths, including schists, gneiss, quartzite, marble, metaturbidite, and metabasalt (Brew & Ford, 1985; Wilson et al., 2015). In Cowee, the Taku metamorphic rocks are more sedimentary in origin, whereas in Herbert, they are largely metavolcanic. Montana Creek includes contributions of both rock types. Peterson (along with the lower reaches of the other watersheds) lies on the Jurassic-Cretaceous sedimentary Gravina belt, which includes graywacke, slate, conglomerate, and breccia (Connor & O'Haire, 1988; Nagorski et al., 2021). Peterson also contains deep (often 2 m) peat deposits of up to 10,000 years (Hood et al., 2020). All watersheds feature Quaternary alluvial and glaciomarine deposits.

2.2. Sample Collection

Streamwater was collected weekly in 2019 ($n = 28$) for the measurement of total suspended sediments (TSS), POC concentration, and δ^{13}C-POC, and monthly ($n = 7$) for Δ^{14}C-POC. Samples for POC and sediment were manually depth integrated by filling 2-L acid leached polycarbonate bottles across the depth profile from a wadable yet well-mixed section of the stream. Rock samples were collected for δ^{13}C analysis to provide the $\delta^{13}C\text{-}POC_{petro}$ endmember. River cobbles large enough to identify bedrock type were collected from the riverbeds of Herbert River, Cowee Creek, and Montana Creek and composited into samples representing the three main bedrock units underlying each watershed: tonalite, Taku terrane, and Gravina belt. In Peterson Creek, Gravina belt rocks were sampled by extracting rock fragments from an outcrop exposed along a bedrock channel section of the stream.

2.3. Chemical Analyses

Concentrations of TSS were quantified by filtering a known volume of water through a pre-weighed, pre-combusted (450°C for >5 hr) Whatman GF/F filter (0.7 μm) in an acid-leached polycarbonate funnel and glass flask vacuum suction filter, followed by drying at 40°C, and reweighing sediment mass. Filters underwent carbonate removal (triple sulfurous acid addition; Connelly et al., 2015) prior to POC and δ^{13}C-POC measurements. Bedrock samples were ashed (6h at 450°C) to remove biospheric carbon and pulverized to >85% passing 75 microns at ALS Geochemistry in Fairbanks, Alaska. Pulverized samples were placed in silver capsules (EA Consumables) and acidified by fumigation with concentrated hydrochloric acid (8 hr). Analysis of δ^{13}C-POC occurred at the UC Davis Stable Isotope Facility with a Micro (for rock endmembers) or EL (for riverine POC samples) Cube elemental analyzer (Elementar Analysensysteme GmbH, Hanau, Germany) connected to an Elementar VisION IRMS. Concentrations of POC (mgL^{-1}) were calculated as the elemental carbon mass divided by the filtered water volume. Samples for Δ^{14}C-POC were filtered onto pre-ashed (6h at 450°C) 47 mm quartz filters (Whatman QM-A), acidified with triple sulfurous acid addition, and oxidized to CO_2 via offline dry combustion with CuO, Cu, and Ag at 850°C in 9 mm quartz tubes at Florida State University. Δ^{14}C was measured at the National Ocean Sciences Atomic Mass Spectrometry (NOSAMS) facility.

2.4. Age-Weight Percent OC Model Calculations

The carbon mass fraction of POC_{bio} was calculated in the riverine POC samples from all four study watersheds following Galy et al. (2008) and Hilton (2017). Briefly,

$$\%OC_{total} \times F_m = \%OC_{total} \times F_{m-bio} - \%OC_{petro} \times F_{m-bio} \quad (1)$$

where $\%OC_{total}$ and $\%OC_{petro}$ are the weight % of the different components of the riverine POC sample, F_m is the radiocarbon activity of a sample, and $F_{m\text{-bio}}$ is the radiocarbon activity of the biospheric endmember. This equation assumes that the combination of POC_{petro} and POC_{bio} equals total POC and that $F_{m\text{-petro}}$ will equal 0 due to petrogenic carbon being older than 50 ka. The model also assumes that $F_{m\text{-bio}}$ is constant across the watersheds. Here, we use this assumption to determine the $F_{m\text{-bio}}$ value integrated across the four watersheds and across the sampling season as a broadly representative experimentally derived biospheric endmember to compare with the petrogenic endmember component. It is beyond the scope of this study to examine how $F_{m\text{-bio}}$ varies in space and time, but future work should focus on illuminating such trends through higher resolution sampling than was

feasible in this study. This data set from all four watersheds demonstrated a strong linear relationship between $\%OC_{total}$ (x) and $\%OC_{total} \times F_m$ (y; Figure S1 in Supporting Information S1), with the equation's slope representing $F_{m\text{-bio}}$ and its intercept expressing $\%OC_{petro} \times F_{m\text{-bio}}$ (Galy et al., 2008). The fraction of POC_{petro} or POC_{bio} in each sample (f_{bio} or f_{petro}, summing to unity) can then be calculated from

$$F_m = f_{bio} \times F_{m-bio+} f_{petro} \times F_{m-petro} \quad (2)$$

with f_{bio} (or f_{petro}) and POC concentration used to calculate the concentration of streamwater POC_{bio} (or POC_{petro}) in mgL^{-1} (Galy et al., 2008). Any f calculated as higher than 1.0 or lower than 0.0 was adjusted to those limits. Flow normalized mean f values were calculated for the four study watersheds using daily streamflow values for each sample date where a value for f was calculated.

2.5. Dual-Isotope Mixing Model

Relative contributions of POC_{bio} and POC_{petro} were also calculated using a two tracer mixing model ($\delta^{13}C$ and $\Delta^{14}C$ of POC) solved using a Markov Chain Monte Carlo method in the MixSIAR package (Stock & Semmens, 2017) in base R (R Core Team, 2019) with each glacierized river sampling treated as a "random" event. MixSIAR estimates source contributions while accounting for uncertainties in source values and residual and process errors (Stock et al., 2018). We limited this modeling technique to the glacierized rivers because non-glacial Peterson Creek receives inputs of organic matter from large salmon runs (Fellman et al., 2009; Hood et al., 2007) and aged peat deposits that can confound the results of the mixing model through their influence on streamwater $\delta^{13}C$-POC and $\Delta^{14}C$-POC values, respectively. Endmember values from the Juneau area, Glacier Bay, and adjacent northern coastal British Columbia for $\delta^{13}C\text{-}POC_{bio}$ ($-28.9 \pm 1.7‰$) and $\Delta^{14}C\text{-}POC_{bio}$ ($39.8 \pm 10.5‰$) were taken from the literature as a representative of vegetation and soil organic matter samples in the study region (Table S1 in Supporting Information S1; Asada et al., 2005; Fellman et al., 2015; Hobbie et al., 1999; Malone et al., 2018). Endmember values for $\delta^{13}C\text{-}POC_{petro}$ were taken from rock samples collected for this study ($-22.36 \pm -3.35‰$; Section 2.3; Section 3.1), while $\Delta^{14}C\text{-}POC_{petro}$ was set at $-1{,}000‰$ due to the lack of radiocarbon activity in rocks older than 50 ka (Goñi et al., 2005; Hilton, 2017) with a standard deviation set to the error in coal standard measurements from NOSAMS. The model was run with endmember means and standard deviations (with n set to the number of samples for whichever variable had fewest samples), and without fractionation since source (not processing) was assessed. The river was included as a random factor (Stock et al., 2018). The model was considered converged when all variables had Gelman-Rubin diagnostics <1.05 (Gelman et al., 2014).

3. Results and Discussion

3.1. Bedrock Characteristics

The endmember rock samples within the study watersheds had distinct chemical and isotopic signatures that allowed us to fingerprint the sources of POC in streamwater. The igneous tonalite samples contained negligible concentrations of OC ($0.02 \pm 0.01\%$OC), while the OC concentrations of the metamorphic Taku terrane and Gravina belt samples were more than an order of magnitude higher (0.34 ± 0.18 and $0.38 \pm 0.22\%$ OC, respectively; Table S2 in Supporting Information S1) and had enriched $\delta^{13}C$-OC values ($-22.03 \pm 1.29‰$ and $-22.94 \pm 3.43‰$, respectively). The carbon-weighted mean $\delta^{13}C$ value for the suite of endmember rock samples was $-22.36‰$ (standard deviation of $3.35‰$). A similar study that focused on coastal watershed POC sources reported endmembers in rocks with a somewhat narrower range in %OC (0.01%–0.29%; Hilton et al., 2008), which can be accounted for by a more homogeneous bedrock source (Mesozoic schists) than occurs in our study region, but with a similar mean ± standard deviation $\delta^{13}C$-OC value ($-21.1 \pm 1.1‰$).

3.2. Suspended Sediment and POC Characteristics

For the runoff season, flow normalized mean POC concentration was highest in heavily glacierized Herbert River ($0.93\ mgL^{-1}$; Table 2) and lowest in lightly glacierized Montana Creek ($0.12\ mgL^{-1}$; Figure S2 in Supporting Information S1 shows seasonal trends). Riverine sediment concentrations and carbon isotopic values for other constituents generally followed the glacierization gradient, with Herbert having the highest flow normalized TSS, most enriched $\delta^{13}C$-POC, and most depleted $\Delta^{14}C$-POC values ($207\ mgL^{-1}$, $-24.0‰$, and $-424‰$, respectively) and Peterson Creek having the lowest flow normalized TSS, most depleted $\delta^{13}C$-POC, and most enriched

Table 2
Flow Normalized Constituent Concentrations and Values for the Study Season, With Ranges of Individual Sampling Events in Parentheses When Present

	POC mgL^{-1}	TSS mgL^{-1}	%OC	TSS:POC	δ^{13}C-POC‰	Δ^{14}C-POC‰
Herbert River	0.93 (0.23–2.3)	207 (7–708)	0.6 (0.3–4.6)	223 (22–370)	−24.0 (−29.8–22.5)	−424 (−594–239)
Cowee Creek	0.29 (0.11–1.65)	12 (1–112)	3.9 (0.6–19.5)	42 (5–167)	−27.6 (−28.8–26.3)	−103 (−256–9)
Montana Creek	0.12 (0.01–0.35)	14 (0–106)	6.7 (0.01–67.1)	589[a] (1–10579)	−27.5 (−30.1–25.6)	−94 (−230–2)
Peterson Creek	0.57 (0.14–1.32)	3 (0–8)	25.9 (5.0–84.9)	4 (1–20)	−27.9 (−31.6–26.3)	7 (−97–15)

[a]235 with the removal of a major outlier during a high flow sediment mobilization event in October.

Δ^{14}C-POC values (3 mgL^{-1}, −27.9‰, and 7‰, respectively). The depletion of δ^{13}C-POC and enrichment of Δ^{14}C-POC with lower glacier coverage is consistent with the idea that ancient petrogenic carbon gives way to modern biospheric carbon as the dominant source of riverine POC shifts with decreasing watershed glacierization (Arimitsu et al., 2018; Hood et al., 2020; Walinsky et al., 2009).

3.3. Riverine POC_{bio} and POC_{petro} Contributions Assessed From Two Models

Using the age-weight percent OC model (Equations 1 and 2; Figure S1 in Supporting Information S1), forested Peterson Creek (Table 1) samples had a flow normalized f_{bio} of 1.00 ± 0.01 (mean ± SE), demonstrating that petrogenic POC was not a meaningful source of OC in the watershed. The mean f_{bio} contribution in lightly glacierized Montana and Cowee Creeks were 0.95 ± 0.03 and 0.94 ± 0.03, respectively. Heavily glacierized Herbert River samples ranged from 0.81 f_{bio} in April before the melt season to as low as 0.43 f_{bio} during peak melt in August with a flow normalized mean of f_{bio} of 0.61 ± 0.05. The flow normalized mean POC_{bio} concentration in the Herbert River (0.70 mgL^{-1}) was the highest of all sites despite the range in Herbert's f_{bio} throughout the melt season (Table 3). The POC_{bio} concentration in forested Peterson Creek was similar to Herbert (0.66 mgL^{-1}), while Montana had the lowest mean flow normalized POC_{bio} concentration (0.09 mgL^{-1}).

Flow normalized mean POC_{petro} concentrations were 0.01 mgL^{-1} for lightly glacierized Montana and Cowee and 0.41 mgL^{-1} for heavily glacierized Herbert. Concentrations of POC_{bio} exceeded concentrations of POC_{petro} for all rivers and sampling events, except in August during peak glacier melt in Herbert (Figure 2; see Section 3.5). Broadly, f_{petro} increased with the glacier melt season as carbon isotopic values for riverine POC in Herbert moved closer to those of the OC-bearing bedrock endmember. An exception to this seasonal pattern occurs in June, when a 9 mm rain event preceding the sample date (Figure S3 in Supporting Information S1) likely flushed a greater fraction of biospheric POC into the stream from the lower, forested reaches of the catchment such that f_{petro} drops, and POC_{bio} is approximately twice that of POC_{petro}. Despite the higher POC_{bio} concentrations present, the substantial contribution of POC_{petro} to the streamwater POC pool in glacierized Herbert supports previous studies highlighting the potential for rock-derived OC export from glacierized watersheds in Southeast Alaska (Cui, Bianchi, Jaeger, & Smith, 2016; Hood et al., 2020). Glacierized fjord sediments in the region have previously been shown to have substantially higher OC_{petro} contributions compared to sediments in unglacierized fjords (Cui,

Table 3
Estimates of f_{petro} and f_{bio} From the Dual-Isotopic Mixing Model and the Age-Weight Percent OC Relationships for Each Watershed, Along With the Concentrations of POC_{bio} and POC_{petro} Calculated From the Age-Weight Percent OC Relationships

	Age-weight percent OC relationship		Dual-isotopic mixing model		Flow normalized POC concentrations and ratios		
	f_{petro}	f_{bio}	f_{petro}	f_{bio}	POC_{bio} mgL^{-1}	POC_{petro} mgL^{-1}	POC_{petro}:POC_{bio}
Herbert River	0.39 ± 0.05	0.61 ± 0.05	0.42 (0.37–0.47)	0.58 (0.53–0.63)	0.70 (0.16–1.41)	0.41 (0.04–0.80)	0.59
Cowee Creek	0.06 ± 0.03	0.94 ± 0.03	0.13 (0.05–0.20)	0.87 (0.81–0.95)	0.25 (0.11–0.42)	0.01 (0.00–0.03)	0.04
Montana Creek	0.05 ± 0.03	0.95 ± 0.03	0.13 (0.04–0.19)	0.87 (0.81–0.96)	0.09 (0.03–0.25)	0.01 (0.00–0.05)	0.11
Peterson Creek	0.00 ± 0.01	1.00 ± 0.01	n/a	n/a	0.66 (0.14–1.32)	0.00 (0.00–0.023)	0.00

Note. The dual-isotopic model results are presented as mean (5%–95% credible intervals) while the age-weight percent OC relationship *f* results are presented as flow normalized mean *f* values ± standard error of *f* values and the flow normalized concentrations are presented with ranges of individual sampling events in parentheses. No ranges are available for flow normalized POC_{petro}:POC_{bio} since that is the single ratio of two flow normalized values.

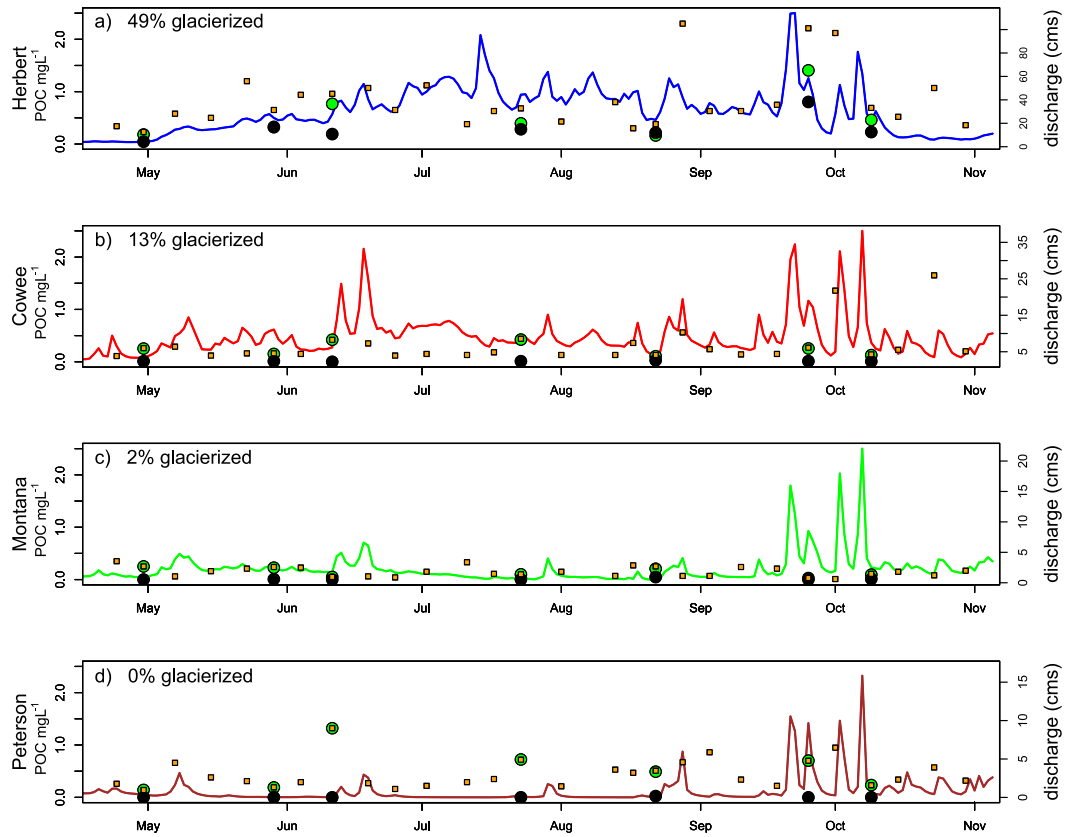

Figure 2. Runoff season POC_{bio} (green) and POC_{petro} (black) concentrations calculated from the age-weight percent OC relationship and measured total particulate organic carbon (small orange squares) versus mean daily discharge in cubic meters per second (cms) for (a) Herbert River, (b) Cowee Creek, (c) Montana Creek, and (d) Peterson Creek.

Bianchi, Jaeger, & Smith, 2016), and here we provide empirical evidence for land-to-ocean export of petrogenic OC from glacierized watersheds.

It is worth noting that ancient biospheric organic matter overridden by past glacial advances and stored beneath the glacier occurs throughout Southeast Alaska (Barclay et al., 2009), and overrun trees have been noted in Herbert (Motyka & Beget, 1996). If ancient overridden biospheric carbon did contribute to POC sources, it could reduce the modeled quantities of both POC_{petro} and POC_{bio}. However, most of the remaining glacier extent in our study watersheds is in high elevation areas that were unlikely subject to Holocene glacier fluctuations that allowed forest development and subsequent overrunning. Furthermore, the low carbon-normalized lignin yields in glacierized rivers in the region (Fellman et al., 2010) suggest that ancient overridden forests do not meaningfully contribute to riverine OC in our study watersheds. We therefore assume two endmembers (biospheric and petrogenic), and the values we present here should be considered the upper limits of possible contributions.

The proportions of biospheric and petrogenic POC derived from the dual-isotope mixing model were relatively similar to those for the age-weighted model. The f_{bio} and credible intervals were nearly identical for Montana and Cowee, but were lower for Herbert (0.58, 0.53–0.63; Table 3). The Montana and Cowee samples grouped in the enriched $\Delta^{14}C$ and more depleted $\delta^{13}C$ region of the isotopic space, overlapping substantially with the vegetation endmember $\delta^{13}C$ values (Figure 3). In contrast, Herbert samples grouped closer to the depleted $\Delta^{14}C$ and enriched $\delta^{13}C$ region of the isotopic space and spread between the vegetation and petrogenic endmembers. For all three glacier rivers, the means and standard errors of f_{bio} and f_{petro} from the age-weight percent model overlapped with the range of the mean and 5%–95% credible intervals for the dual-isotope mixing model. These similar results from the two independent models lend confidence to our results and demonstrate the utility of using either approach for quantifying riverine POC source contributions.

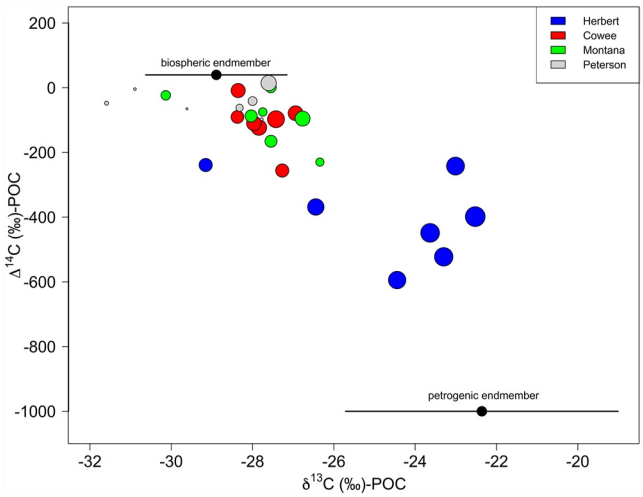

Figure 3. Values of particulate organic carbon in $\Delta^{14}C$ versus $\delta^{13}C$ space. Endmember values are shown with black dots and bars representing the mean and standard deviation of each compilation of petrogenic and biospheric sources (plants and soil organic matter; see Section 2.5; Table S1 in Supporting Information S1). Peterson samples are included as grayed out circles for comparison. Sample dot sizes are scaled by (log (discharge) + 4)/2 to visually represent the four orders of magnitude of the river discharge data cover.

Despite their overall similarity, the dual-isotope mixing model consistently estimated a higher contribution of f_{petro} compared to the age-weight percent model. By using MixSIAR to estimate source contributions, the mixing model incorporates source errors, but a single mean value for the runoff season is calculated, eliminating the possibility of calculating flow-normalized mean values for each sample date. This difference in method may account for the greater attribution of f_{petro} in the dual-isotope model compared to the age-weight percent model. For example, the higher flow events during June and September in Cowee (Figure 2) that appear to have mobilized more POC_{bio} are not accounted for in the straight average while being incorporated into the age-weight percent model's flow-normalized mean values. Since model errors overlapped and were most similar for the heavily glacierized Herbert, which carried the highest concentrations of POC, we discuss POC_{bio} and POC_{petro} calculated from the flow-normalized age-weight model for the remainder of the paper so we can incorporate discharge data.

Across the three glacierized rivers, mean daily flow was positively correlated with concentrations of both POC_{bio} and POC_{petro} (Figure 4a). Mean daily flow was also negatively correlated with f_{bio} and positively correlated with f_{petro} and POC_{petro}:POC_{bio} (Figures 4b and 4c). Bulk POC concentrations for all sampling dates in glacierized watersheds also showed a positive relationship with discharge (adjusted R^2: 0.35; $p < 0.001$; Figure S4a in Supporting Information S1) and TSS (adjusted R^2: 0.72; $p < 0.001$; Figure S4b in Supporting Information S1), while discharge and TSS were also positively correlated (adjusted R^2: 0.40; $p < 0.001$; Figure S4c in Supporting Information S1). Concurrent increases in discharge and POC concentrations imply increased mobilization of POC during high flow conditions, which supports previous work linking yields of POC and water in these glacierized watersheds (Hood et al., 2020). Globally, yields of POC_{bio} and POC_{petro} are correlated with both runoff and suspended sediment yields across a wide variety of watershed types (Galy et al., 2015; Hilton, 2017), matching the general trends seen here. Large rain events mobilize terrestrial material into streams through overland flow as well as through increased soil erosion, which mobilizes POC_{bio} from soil surface layers into streams. Similarly, seasonal and episodic increases in glacial runoff can mobilize subglacial sediments produced by glacial erosion and transport POC_{petro} to rivers.

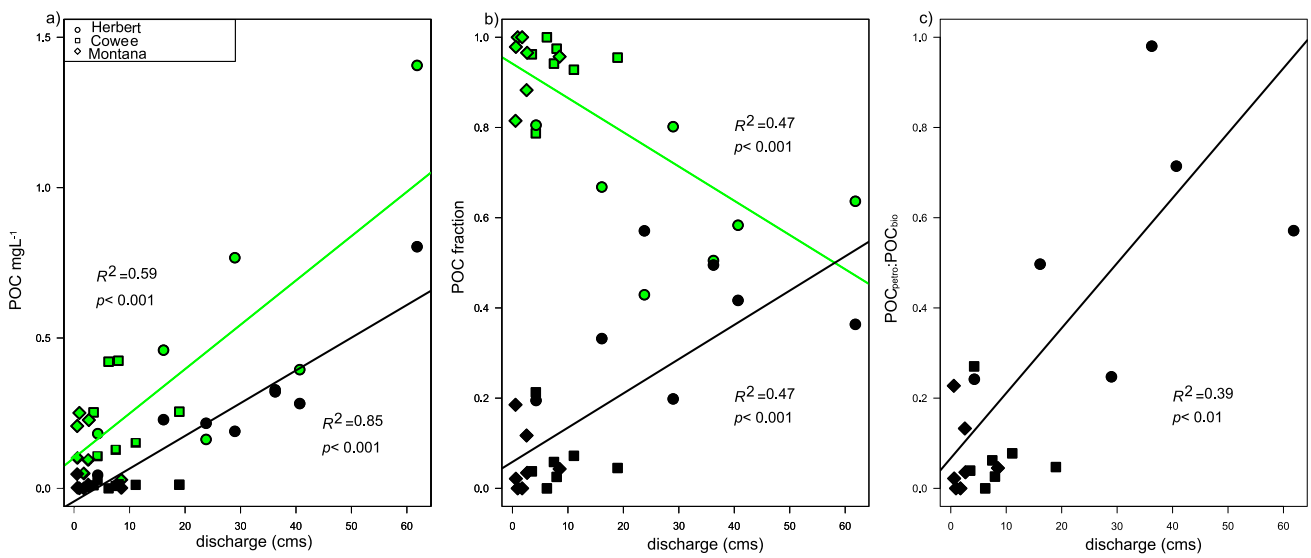

Figure 4. (a) POC_{bio} (green) and POC_{petro} (black) concentrations vs. mean daily discharge for all glacierized rivers combined. (b) f_{bio} (green) and f_{petro} (black) and (c) POC_{petro}:POC_{bio} for each glacierized river sample versus mean daily discharge. Regression lines for each data type shown in green (biospheric) or black (petrogenic, ratio) with adjusted R^2 and p values shown adjacent to each line.

Rivers dominated by glacier runoff can have high sediment and POC yields, which are modulated by bedrock type and exposure to glacier erosion (e.g., Bhatia et al., 2013; Hood et al., 2020). Across the study watersheds, the ratios of flow normalized mean POC_{petro} and POC_{bio} concentrations for each site provide insight into how POC sources shift with changes in watershed glacierization. Heavily glacierized Herbert had a POC_{petro}:POC_{bio} of 0.59 (Table 3), showing that just over a third of riverine POC transported was petrogenic in origin (with flow normalized POC_{petro} and POC_{bio} concentrations of 0.41 and 0.70 mgL^{-1}, respectively; Table 3). Montana and Cowee each had substantially smaller ratios (0.11 and 0.04, respectively), reflecting a predominance of biospheric POC in these watersheds. Few studies incorporate daily flow measurements with POC_{petro} and POC_{bio} concentrations (except see Hilton, 2017), limiting the comparability of flow normalized mean POC_{petro} to POC_{bio} ratios with other environments. The POC_{petro} to POC_{bio} ratios of substantially forested Cowee and Montana (Table 1) are similar to those of temperate, heavily forested watersheds (Hilton, 2017). In contrast, Herbert's ratio falls closest to that of the landslide-prone mountainous Eel River in northern California (0.8), which cuts through tectonically active, OC-bearing bedrock. Herbert has a lower flow normalized POC_{petro}:POC_{bio} than steep, subtropical rivers with warmer temperatures and high precipitation that have high rates of watershed erosion (Hilton, 2017). However, Herbert's mean annual runoff (4.2 myr^{-1}; Hood et al., 2020) is nearly double the reported mean annual runoff of all POC_{petro} bearing rivers in the study that had reported POC_{petro}:POC_{bio} (Hilton, 2017), demonstrating that the combination of high erosion rates and elevated runoff that characterize glacierized watersheds can facilitate substantial lateral export of POC_{petro}.

3.4. Valley Glaciers and POC_{petro} Export

Valley glaciers appear to play a prominent role in bedrock erosion and POC_{petro} transport to downstream and fjord sediments. Here, the heavily glacierized Herbert River watershed contains a major valley-bottom outlet glacier from the Juneau Icefield and has substantially higher flow-normalized f_{petro}, TSS, POC_{petro} concentrations, and POC_{petro}:POC_{bio} ratios than the Montana and Cowee Creek watersheds with their low glacial coverage (Tables 2 and 3). Glacial erosion rates generally increase with ice sliding speed and with ice flux (Hallet et al., 1996; Herman et al., 2015; Koppes et al., 2015), such that the greater velocity and erosive area of the larger Herbert Glacier produce far more rock-derived sediment and POC_{petro} than do the slower velocities and limited erosive areas of the smaller, hanging alpine glaciers present in the other watersheds. The finding that Herbert River has a substantially higher POC_{petro} content compared to Montana and Cowee Creeks suggests that the transition from a larger, highly erosive valley glacier to higher elevation hanging glaciers (rather than simply the presence of ice in a watershed) is an important control on the generation and export of POC_{petro} (Hood et al., 2020).

The modest relationship between f_{petro} and discharge in the glacierized watersheds reflects the relationship between water and sediment export from glaciers (Figure 4b). In un-glacierized watersheds, fluvial hillslope erosion connects POC mobilization directly with water export; however, the processes of water movement and sediment generation are largely decoupled in glacierized watersheds. Glaciers melt primarily from the surface, which drives meltwater discharge at the glacier terminus, but sediment and POC_{petro} generation occurs mainly through subglacial erosion, which is driven by ice dynamics (Hodson et al., 2008). Thus, while glacier melt is important as a transport vector for POC_{petro}, it is not directly involved in producing the sediment it entrains. Glacier meltwater is routed through en- and sub-glacial drainage networks that connect the surface and bed of the glacier. These networks evolve seasonally, from a more distributed system early in the melt season to a more channelized system later in the season, which increases the efficiency of sediment/POC_{petro} removal from previously disconnected regions of the subglacial surface (Chandler et al., 2013; Kohler et al., 2017; Swift et al., 2005).

Bedrock composition can also play a role in decoupling glacier discharge and f_{petro}. In particular, the heterogeneity of OC-bearing bedrock within the area of the catchment subject to glacial erosion is an important control on the generation of POC_{petro}. Sub-glacial bedrock erosion is far more powerful than riverine bedrock erosion downstream (Herman et al., 2015). As a result, the locations of the highest glacial erosion rates, and whether those locations contain OC-bearing bedrock outcrops, ultimately dictate how much POC_{petro} is available for fluvial export. As glaciers continue to retreat over heterogeneous bedrock, POC_{petro} contributions to glacier rivers will shift accordingly.

3.5. Transport and Burial of POC_{bio} by Glacial Rivers

The high concentrations of POC_{bio} reported here in the heavily glacierized Herbert River (which exceeded POC_{petro} concentrations except in August during maximum glacier melt; Figure 2) highlight the importance of glacier watersheds for exporting and potentially contributing to the burial of POC_{bio} in the coastal ocean. It is possible

that rain events, which are common in maritime environments, may be an important driver of POC_{bio} export from glacier watersheds. In particular, the two highest POC_{bio} concentrations we documented in the Hebert River (Figure 2a) occurred coincident with the highest TSS concentrations during 9 and 24 mm rain events in June and September, respectively (Figure S3 in Supporting Information S1). These storms likely mobilized a combination of rock-derived sediments that were eroded by the glacier and washed out by the rain, and, separately, soil organic matter from the unglacierized portion of the catchment, including from non-glacial tributary streams that drain wetlands and forested hillslopes. Thus, rain events can increase both TSS and POC_{bio}. Recently deglaciated terrain that is actively revegetating and developing soil may be another source of the higher POC_{bio} concentrations in Herbert and may be more susceptible to POC_{bio} mobilization during rain events than more mature forests, as has been seen with increased POC export due to forest disturbance (Webster et al., 1990). Thus, storm events on top of underlying glacial melt with a high baseline TSS load may produce a hot moment for the burial of POC_{bio} in downstream fjords. Mineral association of POC in rivers or estuaries (Hemingway et al., 2019) and deposition with large number of sediments can substantially slow the mineralization of POC particularly under anoxic conditions (Peter et al., 2016; Repasch et al., 2021; Richardson et al., 2013). Long-term sedimentation of OC in coastal environments is a critical pathway of carbon sequestration over geologic timescales (Berner, 1982; Hilton, 2017). Glacier-containing fjords in northern Southeast Alaska have high sedimentation rates, with upper Lynn Canal experiencing a mass accumulation rate of 0.58 ± 0.15 g cm^{-2} yr^{-1} and other glacierized fjords reaching 33.5 ± 18 g cm^{-2} yr^{-1} (Walinsky et al., 2009). In contrast, fjords in the southern portion of Southeast Alaska with little or no glacial input had lower mass accumulation rates (0.06–0.19 g cm^{-2} yr^{-1}) (Walinsky et al., 2009). High rates support the possibility of rapid POC_{bio} burial in fjords downstream of glacierized catchments.

Riverine POC transport is not a passive process because a fraction can drive microbial production during riverine transport or in the estuary, which limits burial in downstream depocenters (e.g., Attermeyer et al., 2018; Casper et al., 2015). However, coastal watersheds in Southeast Alaska are characterized by short flow networks, cool temperatures, and rapid transit times, all of which limit POC mineralization during transport to estuaries. In this context, large rainfall events during the glacial melt season could provide high burial potential for both POC_{bio} and POC_{petro} by rapid relocation to coastal sediments and protection by the same mechanism. It is beyond the scope of this study to examine the rates of POC_{bio} and POC_{petro} mineralization during transport and deposition in coastal waters, but such measurements would be necessary to better understand how glacial recession will impact the fate of POC in coastal waters.

Since both TSS and POC_{bio} concentrations are highest in heavily glacierized Herbert, and POC_{bio} concentration does not appear to increase with a decrease in glacier coverage, POC_{bio} burial may decrease with future glacier shrinkage during the primary runoff season. This supports previous research across a similar gradient in glacier coverage (0%–48%) that suggested the impact of glacier-derived sediment on POC_{bio} burial should peak at intermediate catchment glacierization since sediment production and export decrease with lower glacier coverage but the production of POC_{bio} increases as soil carbon stocks develop following glacier loss (Hood et al., 2020). Since glacial loss decreases summertime runoff over the long term (O'Neel et al., 2015; Young et al., 2021), future glacier shrinkage in the coastal mountain watersheds that ring the Gulf of Alaska may eventually lower POC_{bio} concentration and export (a function of concentration and discharge) to coastal waters during the main glacial runoff season.

3.6. POC_{bio} Burial Versus POC_{petro} Oxidation

The understanding of erosion as a global thermostat, by way of silicate weathering, carbonate precipitation, and POC burial that act as carbon sinks on geologic timescales (Berner, 1982; Galy et al., 2015), has been complicated by the realization that substantial petrogenic OC release as CO_2 can occur during mountain glaciation, weathering, and erosion (Blattmann, 2022; Horan et al., 2017). In mountainous watersheds in New Zealand, for example, enhanced oxidation rates of OC_{petro} during weathering were observed in a watershed with 58% glacier coverage compared with a watershed with 10% glacier coverage, suggesting that glacier recession could result in a net increase in carbon storage in fjords, although this effect is likely dependent on the bedrock lithology and OC content (Horan et al., 2017). In contrast to that, our findings suggest that high sediment production derived from low OC-bearing rocks and export by valley glaciers enables greater POC_{bio} transport and therefore a potential for greater burial and mineral protection in offshore sediments than would be present without glacial inputs. Future work on OC_{petro} oxidation rates in our study watersheds could elucidate CO_2 release due to glaciation and help quantify the net watershed-scale carbon budget.

3.7. Impact of Glacial Retreat on Other Pathways of POC Generation

Glacier retreat decreases physical erosion, water yields, and riverine sediment transport, all of which play a role in POC production and export. However, diminished glacier coverage may stimulate catchment POC production via alternative mechanisms including landslide generation (Dai et al., 2020) and a relative increase in the proportion of streamwater POC derived from lowland peat deposits. In particular, the loss of structural support provided by glacial ice (i.e., debuttressing) as well as from permafrost degradation can lead to an increase in the landslide activity within actively deglaciating, oversteepened valleys, as has been observed in Alaska (Dai et al., 2020), the European Alps (Kos et al., 2016), and Asian Himalayas (Liu et al., 2021). Landslides are common in glacierized and forested catchments in the coastal mountains ringing the Gulf of Alaska (Dai et al., 2020; Guthrie et al., 2010; Vascik et al., 2021). In this study, the influence of landslide activity on watershed POC export is most evident in the lightly glacierized Montana Creek catchment, which contains several recent landslides in the upper reaches of the catchment (Figure S5 in Supporting Information S1). Landslides play a major role in controlling the relationship between sediment and POC concentration (Hilton et al., 2008). This may explain the extremely high mean flow normalized ratio of TSS to POC concentration (TSS:POC) in Montana of 589 (Table 2). For the other watersheds, the mean flow normalized TSS:POC followed increasing glacierization (Peterson: 4; Cowee: 42; and Herbert: 223; Table 2), aligning with previous research showing that catchment sediment:POC increases from greater biospheric POC contribution toward greater rock-derived POC contribution (Hilton, 2017; Hood et al., 2020). The elevated flow normalized TSS:POC in Montana (589) was strongly influenced by a single datapoint from an early October storm where Montana discharge and TSS were high (105.8 mgL^{-1}) and POC was low (0.01 mgL^{-1}). This could have coincided with a landslide sediment mobilization event. Excluding this outlier event, the flow normalized TSS:POC (235) still exceeded that for the other three study watersheds. In this context, landslides have the potential to increase their relative control over POC and sediment mobilization within steep glacierized watersheds due to an increase in frequency combined with a decrease in glacier erosion as catchment ice disappears (Dai et al., 2020; Hallet et al., 1996).

With reduced glacial melt contribution to streamflow, discharge from peatland-dominated tributaries will increase in importance, allowing for the signal of ancient peat degradation to increase where wetlands are present. Radiocarbon dates for ~1 m deep peatland samples near the study watersheds show ages from ~1,300 to 2600 years old, while deeper peat samples have reached >10,000 years old in watersheds with extensive peat deposits (Payne & Blackford, 2008). In this study, moderately aged POC values (up to ~800 years old) in Peterson suggest inputs from old peat in substantial wetlands in the watersheds (Table 1). Warm and dry conditions can lower soil water tables, leading to increased OC decomposition and release of peatland organic carbon as partial decomposition products (Fenner & Freeman, 2011; Wilson et al., 2016). The 2019 study period was warm and dry for the Juneau area, with April-October all receiving below average precipitation and May-August being above average temperature based on weather station observations (Table S3 in Supporting Information S1; NOAA, 2019). The Δ^{14}C-POC values for Peterson reached −97.4‰ (~750 years old) and multiple samples had Δ^{14}C-POC values below −60‰ (or >400 years old) during low flow, drier periods, while modern Δ^{14}C-POC values occurred during high flow events mobilizing fresh plant material. Future regional warming may exacerbate the decomposition of deep peat and the contribution of old peatland carbon to riverine POC loads in forested watersheds like Peterson as well as the lower, forested reaches of larger glacierized watersheds like Herbert and Cowee.

3.8. Global Glacial Retreat and Riverine POC Dynamics

Globally, mountain glaciers are predicted to lose 26%–41% of their 2006 volume by 2100, with a concomitant ~20% decrease in glacial runoff (Bliss et al., 2014; Radić et al., 2014; Rounce et al., 2023). A similar decrease in POC_{petro} export from deglacierized watersheds around the world therefore appears probable through two mechanisms. The ongoing shift to smaller, slower moving alpine glaciers will likely lower bedrock erosion rates (Hallet et al., 1996; Koppes et al., 2015), decreasing the production of sediment and POC_{petro}, thereby lowering riverine POC_{petro} concentrations. At the same time, decreased glacier runoff and a switch from a glacial melt dominated annual hydrograph to one dominated mainly by snow or rain inputs (Bliss et al., 2014; Giesbrecht et al., 2022) will decrease catchment water yields and the overall riverine flux of POC_{petro}, particularly during midsummer when glacier melt and erosion peak.

If the patterns in POC_{bio} concentration and POC_{petro}:POC_{bio} ratios observed across our glacierized watersheds are broadly reflective of the shifts in POC provenance that can be expected as glaciers recede, future decreases

in glacial runoff (Bliss et al., 2014) may lead to lower average riverine POC_{petro}:POC_{bio} ratios and a greater fraction of POC exported as POC_{bio} from currently glacierized regions (e.g., the Gulf of Alaska, Patagonia, the Himalaya, Scandinavia, the Alps, and the high Arctic; Armstrong et al., 2005). This would mean a higher percentage of recently fixed carbon present in the bulk POC pool that is exported to coastal environments around the world. However, with lower summer discharge from glacier loss, lower overall fluxes of POC_{bio} may be transported out of deglacierizing watersheds. High sediment yields are common in glacierized watersheds (Hallet et al., 1996) and decrease the oxidation of POC in the water column and in the sediments through higher POC burial (Canfield, 1994; Galy et al., 2015). Glacier loss is accompanied by decreasing suspended sediments, whose absence may thus shrink the ability of proglacial fjords to store and protect POC_{bio}, particularly in glacierized regions like Patagonia where decreasing annual precipitation and increasing extreme drought events have been predicted (Aguayo et al., 2019). Alternatively, in regions such as the Hindu Kush Himalaya and Southeast Alaska where high-intensity precipitation events are forecast to increase (Lader et al., 2022; Sabin et al., 2020), event-based suspended sediment export or landslide events and concomitant sediment mobilization may become greater as well (Guthrie et al., 2010). This could increase sediment availability for exported POC_{bio} protection in downstream fjords (e.g., Glacier Bay; Walinsky et al., 2009) or deltas (e.g., the Bengal fan; Galy et al., 2007).

The shifting ratios of POC_{petro} and POC_{bio} in deglacierizing rivers may also impact in-stream POC degradation. Kerogen dominates POC_{petro} and has long been viewed as recalcitrant due to its stable molecular structure and mineral-associated physical protection (Guillemette et al., 2017). The mineral associations seen with ancient POC of likely petrogenic origin in watersheds undergoing glacial retreat imply a high likelihood of protection against microbial consumption (Bröder et al., 2022), though recently OC_{petro} has been shown to fuel some microbial production both in soils and fjord sediments (Hemingway et al., 2018; Ruben et al., 2023). Its utility to in-stream production remains unclear and is likely relatively small given the substantial amounts of POC_{petro} that make it into coastal sediments (Cui, Bianchi, Jaeger, & Smith, 2016). In contrast, contemporary POC_{bio} can undergo active degradation in the water column, including after entry into the ocean (Attermeyer et al., 2018; Vonk et al., 2014), though in general autochthonous POC such as algae or biofilms are more bioavailable to higher trophic levels than terrestrially derived POC (Brett et al., 2017; Guo et al., 2016). It appears possible that with glacier retreat, a higher fraction of exported POC could fuel food webs and increase in-stream POC degradation, though the overall flux of bioavailable POC could decrease during the summer melt season with diminished discharge. It is therefore not clear how modern biospheric POC flux and consequent burial or food web incorporation will shift global riverine carbon balances with continued watershed deglacierization.

Data Availability Statement

All data used in this study are freely available on the Open Science Framework M. I. Behnke (2023) (https://osf.io/x4b27/; https://doi.org/10.17605/OSF.IO/X4B27).

Acknowledgments
The authors would like to thank Emily Whitney, Connor Johnson, Mollie Dwyer, Sol Martinez for assistance with field and laboratory work. Funding was provided by the U.S. National Science Foundation grants through the Coastal Margins Research Coordination Network (DEB-1557186) and Alaska EPSCoR (OIA-1757348). This work took place in Lingít Aaní on the lands of the Aak'w Kwáan.

References

Aguayo, R., León-Muñoz, J., Vargas-Baecheler, J., Montecinos, A., Garreaud, R., Urbina, M., et al. (2019). The glass half-empty: Climate change drives lower freshwater input in the coastal system of the Chilean Northern Patagonia. *Climatic Change*, *155*(3), 417–435. https://doi.org/10.1007/s10584-019-02495-6

Arimitsu, M. L., Hobson, K. A., Webber, D. A. N., Piatt, J. F., Hood, E. W., & Fellman, J. B. (2018). Tracing biogeochemical subsidies from glacier runoff into Alaska's coastal marine food webs. *Global Change Biology*, *24*(1), 387–398. https://doi.org/10.1111/gcb.13875

Armstrong, R., Raup, B., Khalsa, S., Barry, R., Kargel, J., Helm, C., & Kieffer, H. (2005). *GLIMS glacier database*. National Snow and Ice Data Center. Digital media.

Asada, T., Warner, B., & Aravena, R. (2005). Effects of the early stage of decomposition on change in carbon and nitrogen isotopes in Sphagnum litter. *Journal of Plant Interactions*, *1*(4), 229–237. https://doi.org/10.1080/17429140601056766

Attermeyer, K., Catalán, N., Einarsdottir, K., Freixa, A., Groeneveld, M., Hawkes, J. A., et al. (2018). Organic carbon processing during transport through boreal inland waters: Particles as important sites. *Journal of Geophysical Research: Biogeosciences*, *123*(8), 2412–2428. https://doi.org/10.1029/2018JG004500

Barclay, D. J., Wiles, G. C., & Calkin, P. E. (2009). Holocene glacier fluctuations in Alaska. *Quaternary Science Reviews*, *28*(21–22), 2034–2048. https://doi.org/10.1016/j.quascirev.2009.01.016

Behnke, M. I. (2023). The role of glacier erosion in riverine particulate organic carbon export. https://doi.org/10.17605/OSF.IO/X4B27

Berg, S., Jivcov, S., Kusch, S., Kuhn, G., White, D., Bohrmann, G., et al. (2021). Increased petrogenic and biospheric organic carbon burial in sub-Antarctic fjord sediments in response to recent glacier retreat. *Limnology & Oceanography*, *66*(12), 4347–4362. https://doi.org/10.1002/lno.11965

Berner, R. A. (1982). Burial of organic carbon and pyrite sulfur in the modern ocean: Its geochemical and environmental significance. *American Journal of Science*, *282*(4), 282–473. https://doi.org/10.2475/ajs.282.4.451

Berthier, E., Larsen, C., Durkin, W. J., Willis, M. J., & Pritchard, M. E. (2018). Brief communication: Unabated wastage of the Juneau and Stikine icefields (southeast Alaska) in the early 21st century. *The Cryosphere*, *12*(4), 1523–1530. https://doi.org/10.5194/tc-12-1523-2018

Bhatia, M. P., Das, S. B., Xu, L., Charette, M. A., Wadham, J. L., & Kujawinski, E. B. (2013). Organic carbon export from the Greenland ice sheet. *Geochimica et Cosmochimica Acta*, *109*, 329–344. https://doi.org/10.1016/j.gca.2013.02.006

Blattmann, T. M. (2022). Ideas and perspectives: Emerging contours of a dynamic exogenous kerogen cycle. *Biogeosciences*, *19*(2), 359–373. https://doi.org/10.5194/bg-19-359-2022

Bliss, A., Hock, R., & Radić, V. (2014). Global response of glacier runoff to twenty-first century climate change. *J Geophys ResEarth Surface*, *119*(4), 717–730. https://doi.org/10.1002/2013jf002931

Bogen, J. (2008). *The impact of climate change on glacial sediment delivery to rivers* (Vol. 325, p. 432). IAHS publication.

Brett, M. T., Bunn, S. E., Chandra, S., Galloway, A. W. E., Guo, F., Kainz, M. J., et al. (2017). How important are terrestrial organic carbon inputs for secondary production in freshwater ecosystems? *Freshwater Biology*, *62*(5), 833–853. https://doi.org/10.1111/fwb.12909

Brew, D. A., & Ford, A. B. (1985). *Preliminary reconnaissance geologic map of the Juneau, Taku river, Atlin, and part of the Skagway 1: 250,000 quadrangles, southeastern Alaska*. US Geological Survey.

Bröder, L., Hirst, C., Opfergelt, S., Thomas, M., Vonk, J. E., Haghipour, N., et al. (2022). Contrasting export of particulate organic carbon from Greenlandic glacial and nonglacial streams. *Geophysical Research Letters*, *49*(21), e2022GL101210. https://doi.org/10.1029/2022gl101210

Buma, B., & Barrett, T. M. (2015). Spatial and topographic trends in forest expansion and biomass change, from regional to local scales. *Global Change Biology*, *21*(9), 3445–3454. https://doi.org/10.1111/gcb.12915

Canfield, D. E. (1994). Factors influencing organic carbon preservation in marine sediments. *Chemical Geology*, *114*(3–4), 315–329. https://doi.org/10.1016/0009-2541(94)90061-2

Casper, A. F., Rautio, M., Martineau, C., & Vincent, W. (2015). Variation and assimilation of Arctic riverine sestonin the pelagic food web of the Mackenzie river delta and Beaufort sea transition Zone. *Estuaries and Coasts*, *38*(5), 1656–1663. https://doi.org/10.1007/s12237-014-9917-z

Chandler, D., Wadham, J., Lis, G., Cowton, T., Sole, A., Bartholomew, I., et al. (2013). Evolution of the subglacial drainage system beneath the Greenland Ice Sheet revealed by tracers. *Nature Geoscience*, *6*(3), 195–198. https://doi.org/10.1038/ngeo1737

Connelly, T. L., McClelland, J. W., Crump, B. C., Kellogg, C. T., & Dunton, K. H. (2015). Seasonal changes in quantity and composition of suspended particulate organic matter in lagoons of the Alaskan Beaufort Sea. *Marine Ecology Progress Series*, *527*, 31–45. https://doi.org/10.3354/meps11207

Connor, C., & O'Haire, D. (1988). *Roadside geology of Alaska*. Mountain Press Publishing Company.

Cui, X., Bianchi, T. S., Jaeger, J. M., & Smith, R. W. (2016). Biospheric and petrogenic organic carbon flux along southeast Alaska. *Earth and Planetary Science Letters*, *452*, 238–246. https://doi.org/10.1016/j.epsl.2016.08.002

Cui, X., Bianchi, T. S., Savage, C., & Smith, R. W. (2016). Organic carbon burial in fjords: Terrestrial versus marine inputs. *Earth and Planetary Science Letters*, *451*, 41–50. https://doi.org/10.1016/j.epsl.2016.07.003

Dai, C., Higman, B., Lynett, P. J., Jacquemart, M., Howat, I. M., Liljedahl, A. K., et al. (2020). Detection and assessment of a large and potentially tsunamigenic periglacial landslide in Barry Arm, Alaska. *Geophysical Research Letters*, *47*(22), e2020GL089800. https://doi.org/10.1029/2020gl089800

Delaney, I., & Adhikari, S. (2020). Increased subglacial sediment discharge in a warming climate: Consideration of ice dynamics, glacial erosion, and fluvial sediment transport. *Geophysical Research Letters*, *47*(7), e2019GL085672. https://doi.org/10.1029/2019gl085672

Dethier, E. N., Renshaw, C. E., & Magilligan, F. J. (2022). Rapid changes to global river suspended sediment flux by humans. *Science*, *376*(6600), 1447–1452. https://doi.org/10.1126/science.abn7980

Fellman, J. B., Hood, E., D'Amore, D. V., Edwards, R. T., & White, D. (2009). Seasonal changes in the chemical quality and biodegradability of dissolved organic matter exported from soils to streams in coastal temperate rainforest watersheds. *Biogeochemistry*, *95*(2–3), 277–293. https://doi.org/10.1007/s10533-009-9336-6

Fellman, J. B., Hood, E., Raymond, P. A., Hudson, J., Bozeman, M., & Arimitsu, M. (2015). Evidence for the assimilation of ancient glacier organic carbon in a proglacial stream food web. *Limnology & Oceanography*, *60*(4), 1118–1128. https://doi.org/10.1002/lno.10088

Fellman, J. B., Nagorski, S., Pyare, S., Vermilyea, A. W., Scott, D., & Hood, E. (2014). Stream temperature response to variable glacier coverage in coastal watersheds of Southeast Alaska. *Hydrological Processes*, *28*(4), 2062–2073. https://doi.org/10.1002/hyp.9742

Fellman, J. B., Spencer, R. G., Hernes, P. J., Edwards, R. T., D'Amore, D. V., & Hood, E. (2010). The impact of glacier runoff on the biodegradability and biochemical composition of terrigenous dissolved organic matter in near-shore marine ecosystems. *Marine Chemistry*, *121*(1–4), 112–122. https://doi.org/10.1016/j.marchem.2010.03.009

Fenner, N., & Freeman, C. (2011). Drought-induced carbon loss in peatlands. *Nature Geoscience*, *4*(12), 895–900. https://doi.org/10.1038/ngeo1323

Galy, V., Beyssac, O., France-Lanord, C., & Eglinton, T. (2008). Recycling of graphite during Himalayan erosion: A geological stabilization of carbon in the crust. *Science*, *322*(5903), 943–945. https://doi.org/10.1126/science.1161408

Galy, V., France-Lanord, C., Beyssac, O., Faure, P., Kudrass, H., & Palhol, F. (2007). Efficient organic carbon burial in the Bengal fan sustained by the Himalayan erosional system. *Nature*, *450*(7168), 407–410. https://doi.org/10.1038/nature06273

Galy, V., Peucker-Ehrenbrink, B., & Eglinton, T. (2015). Global carbon export from the terrestrial biosphere controlled by erosion. *Nature*, *521*(7551), 204–207. https://doi.org/10.1038/nature14400

Gelman, A., Carlin, J. B., Stern, H. S., & Rubin, D. B. (2014). *Bayesian data analysis* (Vol. 2). Taylor & Francis.

Giesbrecht, I. J., Tank, S. E., Frazer, G. W., Hood, E., Gonzalez Arriola, S. G., Butman, D. E., et al. (2022). Watershed classification predicts streamflow regime and organic carbon dynamics in the Northeast Pacific coastal temperate rainforest. *Global Biogeochemical Cycles*, *36*(2), e2021GB007047. https://doi.org/10.1029/2021gb007047

Goñi, M. A., Yunker, M. B., Macdonald, R. W., & Eglinton, T. I. (2005). The supply and preservation of ancient and modern components of organic carbon in the Canadian Beaufort Shelf of the Arctic Ocean. *Marine Chemistry*, *93*(1), 53–73. https://doi.org/10.1016/j.marchem.2004.08.001

Guillemette, F., Bianchi, T. S., & Spencer, R. G. (2017). Old before your time: Ancient carbon incorporation in contemporary aquatic foodwebs. *Limnology & Oceanography*, *62*(4), 1682–1700. https://doi.org/10.1002/lno.10525

Guo, F., Kainz, M. J., Sheldon, F., & Bunn, S. E. (2016). The importance of high-quality algal food sources in stream food webs–current status and future perspectives. *Freshwater Biology*, *61*(6), 815–831. https://doi.org/10.1111/fwb.12755

Guthrie, R., Mitchell, S., Lanquaye-Opoku, N., & Evans, S. (2010). Extreme weather and landslide initiation in coastal British Columbia. *The Quarterly Journal of Engineering Geology and Hydrogeology*, *43*(4), 417–428. https://doi.org/10.1144/1470-9236/08-119

Hallet, B., Hunter, L., & Bogen, J. (1996). Rates of erosion and sediment evacuation by glaciers: A review of field data and their implications. *Global and Planetary Change*, *12*(1–4), 213–235. https://doi.org/10.1016/0921-8181(95)00021-6

Hedges, J. I. (1992). Global biogeochemical cycles: Progress and problems. *Marine Chemistry*, *39*(1–3), 67–93. https://doi.org/10.1016/0304-4203(92)90096-s

Hemingway, J. D., Hilton, R. G., Hovius, N., Eglinton, T. I., Haghipour, N., Wacker, L., et al. (2018). Microbial oxidation of lithospheric organic carbon in rapidly eroding tropical mountain soils. *Science*, *360*(6385), 209–212. https://doi.org/10.1126/science.aao6463
Hemingway, J. D., Rothman, D. H., Grant, K. E., Rosengard, S. Z., Eglinton, T. I., Derry, L. A., & Galy, V. V. (2019). Mineral protection regulates long-term global preservation of natural organic carbon. *Nature*, *570*(7760), 228–231. https://doi.org/10.1038/s41586-019-1280-6
Herman, F., Beyssac, O., Brughelli, M., Lane, S. N., Leprince, S., Adatte, T., et al. (2015). Erosion by an alpine glacier. *Science*, *350*(6257), 193–195. https://doi.org/10.1126/science.aab2386
Hilton, R. G. (2017). Climate regulates the erosional carbon export from the terrestrial biosphere. *Geomorphology*, *277*, 118–132. https://doi.org/10.1016/j.geomorph.2016.03.028
Hilton, R. G., Galy, A., & Hovius, N. (2008). Riverine particulate organic carbon from an active mountain belt: Importance of landslides. *Global Biogeochemical Cycles*, *22*(1). https://doi.org/10.1029/2006gb002905
Hilton, R. G., & West, A. J. (2020). Mountains, erosion and the carbon cycle. *Nature Reviews Earth & Environment*, *1*(6), 284–299. https://doi.org/10.1038/s43017-020-0058-6
Hobbie, E. A., Macko, S. A., & Shugart, H. H. (1999). Insights into nitrogen and carbon dynamics of ectomycorrhizal and saprotrophic fungi from isotopic evidence. *Oecologia*, *118*(3), 353–360. https://doi.org/10.1007/s004420050736
Hodson, A., Anesio, A. M., Tranter, M., Fountain, A., Osborn, M., Priscu, J., et al. (2008). Glacial ecosystems. *Ecological Monographs*, *78*(1), 41–67. https://doi.org/10.1890/07-0187.1
Hood, E., Fellman, J., & Edwards, R. T. (2007). Salmon influences on dissolved organic matter in a coastal temperate brownwater stream: An application of fluorescence spectroscopy. *Limnology & Oceanography*, *52*(4), 1580–1587. https://doi.org/10.4319/lo.2007.52.4.1580
Hood, E., Fellman, J. B., & Spencer, R. G. (2020). Glacier loss impacts riverine organic carbon transport to the ocean. *Geophysical Research Letters*, *47*(19), e2020GL089804. https://doi.org/10.1029/2020gl089804
Horan, K., Hilton, R. G., Selby, D., Ottley, C. J., Gröcke, D. R., Hicks, M., & Burton, K. W. (2017). Mountain glaciation drives rapid oxidation of rock-bound organic carbon. *Science Advances*, *3*(10), e1701107. https://doi.org/10.1126/sciadv.1701107
Kirschbaum, M. U., Zeng, G., Ximenes, F., Giltrap, D. L., & Zeldis, J. R. (2019). Towards a more complete quantification of the global carbon cycle. *Biogeosciences*, *16*(3), 831–846. https://doi.org/10.5194/bg-16-831-2019
Kohler, T. J., Žárský, J., Yde, J., Lamarche-Gagnon, G., Hawkings, J. R., Tedstone, A. J., et al. (2017). Carbon dating reveals a seasonal progression in the source of particulate organic carbon exported from the Greenland Ice Sheet. *Geophysical Research Letters*, *44*(12), 6209–6217. https://doi.org/10.1002/2017gl073219
Koppes, M., Hallet, B., Rignot, E., Mouginot, J., Wellner, J. S., & Boldt, K. (2015). Observed latitudinal variations in erosion as a function of glacier dynamics. *Nature*, *526*(7571), 100–103. https://doi.org/10.1038/nature15385
Kos, A., Amann, F., Strozzi, T., Delaloye, R., von Ruette, J., & Springman, S. (2016). Contemporary glacier retreat triggers a rapid landslide response, Great Aletsch Glacier, Switzerland. *Geophysical Research Letters*, *43*(24), 12466–412474. https://doi.org/10.1002/2016gl071708
Lader, R., Bhatt, U. S., Walsh, J. E., & Bieniek, P. A. (2022). Projections of hydroclimatic extremes in Southeast Alaska under the RCP8. 5 scenario. *Earth Interactions*, *26*(1), 180–194. https://doi.org/10.1175/ei-d-21-0023.1
Liu, J., Wu, Y., & Gao, X. (2021). Increase in occurrence of large glacier-related landslides in the high mountains of Asia. *Scientific Reports*, *11*, 1–12. https://doi.org/10.1038/s41598-021-81212-9
Malone, E. T., Abbott, B. W., Klaar, M. J., Kidd, C., Sebilo, M., Milner, A. M., & Pinay, G. (2018). Decline in ecosystem δ13C and mid-successional nitrogen loss in a two-century postglacial chronosequence. *Ecosystems*, *21*(8), 1659–1675. https://doi.org/10.1007/s10021-018-0245-1
Milner, A. M., Khamis, K., Battin, T. J., Brittain, J. E., Barrand, N. E., Füreder, L., et al. (2017). Glacier shrinkage driving global changes in downstream systems. *Proceedings of the National Academy of Sciences of the United States of America*, *114*(37), 9770–9778. https://doi.org/10.1073/pnas.1619807114
Motyka, R. J., & Beget, J. E. (1996). Taku Glacier, southeast Alaska, USA: Late Holocene history of a tidewater glacier. *Arctic and Alpine Research*, *28*(1), 42–51. https://doi.org/10.2307/1552084
Nagorski, S. A., Vermilyea, A. W., & Lamborg, C. H. (2021). Mercury export from glacierized Alaskan watersheds as influenced by bedrock geology, watershed processes, and atmospheric deposition. *Geochimica et Cosmochimica Acta*, *304*, 32–49. https://doi.org/10.1016/j.gca.2021.04.003
NOAA. (2019). National centers of environmental information climate data online search.
O'Neel, S., Hood, E., Bidlack, A. L., Fleming, S. W., Arimitsu, M. L., Arendt, A., et al. (2015). Icefield-to-ocean linkages across the northern Pacific coastal temperate rainforest ecosystem. *BioScience*, *65*(5), 499–512. https://doi.org/10.1093/biosci/biv027
Payne, R., & Blackford, J. (2008). Peat humification and climate change: A multi-site comparison from mires in South-East Alaska. *Mires & Peat*, 1–11.
Peter, S., Isidorova, A., & Sobek, S. (2016). Enhanced carbon loss from anoxic lake sediment through diffusion of dissolved organic carbon. *Journal of Geophysical Research: Biogeosciences*, *121*(7), 1959–1977. https://doi.org/10.1002/2016jg003425
Radić, V., Bliss, A., Beedlow, A. C., Hock, R., Miles, E., & Cogley, J. G. (2014). Regional and global projections of twenty-first century glacier mass changes in response to climate scenarios from global climate models. *Climate Dynamics*, *42*(1–2), 37–58. https://doi.org/10.1007/s00382-013-1719-7
R Core Team. (2019). *R: A language and environment for statistical computing*. R Foundation for Statistical Computing.
Repasch, M., Scheingross, J. S., Hovius, N., Lupker, M., Wittmann, H., Haghipour, N., et al. (2021). Fluvial organic carbon cycling regulated by sediment transit time and mineral protection. *Nature Geoscience*, *14*(11), 1–7. https://doi.org/10.1038/s41561-021-00845-7
Richardson, D. C., Newbold, J. D., Aufdenkampe, A. K., Taylor, P. G., & Kaplan, L. A. (2013). Measuring heterotrophic respiration rates of suspended particulate organic carbon from stream ecosystems. *Limnology and Oceanography: Methods*, *11*(5), 247–261. https://doi.org/10.4319/lom.2013.11.247
Rounce, D. R., Hock, R., Maussion, F., Hugonnet, R., Kochtitzky, W., Huss, M., et al. (2023). Global glacier change in the 21st century: Every increase in temperature matters. *Science*, *379*(6627), 78–83. https://doi.org/10.1126/science.abo1324
Ruben, M., Hefter, J., Schubotz, F., Geibert, W., Butzin, M., Gentz, T., et al. (2023). Fossil organic carbon utilization in marine Arctic fjord sediments by subsurface micro-organisms. *Nature Geoscience*, *16*(7), 1–6. https://doi.org/10.1038/s41561-023-01198-z
Sabin, T., Krishnan, R., Vellore, R., Priya, P., Borgaonkar, H., Singh, B. B., & Sagar, A. (2020). Climate change over the Himalayas. In *Assessment of climate change over the Indian region: A report of the ministry of earth Sciences (MoES)* (pp. 207–222). Government of India.
Smith, R. W., Bianchi, T. S., Allison, M., Savage, C., & Galy, V. (2015). High rates of organic carbon burial in fjord sediments globally. *Nature Geoscience*, *8*(6), 450–453. https://doi.org/10.1038/ngeo2421
Smith, T. M., Cramer, W., Dixon, R., Leemans, R., Neilson, R., & Solomon, A. (1993). The global terrestrial carbon cycle. *Water, Air, and Soil Pollution*, *70*(1–4), 19–37. https://doi.org/10.1007/bf01104986
Stock, B., & Semmens, B. (2017). MixSIAR GUI user manual v3. 1.

Stock, B. C., Jackson, A. L., Ward, E. J., Parnell, A. C., Phillips, D. L., & Semmens, B. X. (2018). Analyzing mixing systems using a new generation of Bayesian tracer mixing models. *PeerJ*, *6*, e5096. https://doi.org/10.7717/peerj.5096

Swift, D. A., Nienow, P. W., & Hoey, T. B. (2005). Basal sediment evacuation by subglacial meltwater: Suspended sediment transport from haut glacier d'Arolla, Switzerland. *Earth Surface Processes and Landforms*, *30*(7), 867–883. https://doi.org/10.1002/esp.1197

Vascik, B. A., Booth, A. M., Buma, B., & Berti, M. (2021). Estimated amounts and rates of carbon mobilized by landsliding in old-growth temperate forests of SE Alaska. *Journal of Geophysical Research: Biogeosciences*, *126*(11), e2021JG006321. https://doi.org/10.1029/2021jg006321

Vonk, J. E., Semiletov, I. P., Dudarev, O. V., Eglinton, T. I., Andersson, A., Shakhova, N., et al. (2014). Preferential burial of permafrost-derived organic carbon in Siberian-Arctic shelf waters. *Journal of Geophysical Research: Oceans*, *119*(12), 8410–8421. https://doi.org/10.1002/2014JC010261

Walinsky, S., Prahl, F., Mix, A., Finney, B., Jaeger, J., & Rosen, G. (2009). Distribution and composition of organic matter in surface sediments of coastal Southeast Alaska. *Continental Shelf Research*, *29*(13), 1565–1579. https://doi.org/10.1016/j.csr.2009.04.006

Webster, J., Golladay, S., Benfield, E., D'Angelo, D., & Peters, G. (1990). Effects of forest disturbance on particulate organic matter budgets of small streams. *Journal of the North American Benthological Society*, *9*(2), 120–140. https://doi.org/10.2307/1467446

Wilson, F. H., Hults, C. P., Mull, C. G., & Karl, S. M. (2015). *Geologic map of Alaska: U.S. Geological Survey Scientific investigations map 3340*. US Department of the Interior, US Geological Survey. https://doi.org/10.3133/sim3340

Wilson, R., Hopple, A., Tfaily, M., Sebestyen, S. D., Schadt, C. W., Pfeifer-Meister, L., et al. (2016). Stability of peatland carbon to rising temperatures. *Nature Communications*, *7*, 1–10. https://doi.org/10.1038/ncomms13723

Young, J. C., Pettit, E., Arendt, A., Hood, E., Liston, G. E., & Beamer, J. (2021). A changing hydrological regime: Trends in magnitude and timing of glacier ice melt and glacier runoff in a high latitude coastal watershed. *Water Resources Research*, *57*(7), e2020WR027404. https://doi.org/10.1029/2020wr027404

Ziemen, F. A., Hock, R., Aschwanden, A., Khroulev, C., Kienholz, C., Melkonian, A., & Zhang, J. (2016). Modeling the evolution of the Juneau icefield between 1971 and 2100 using the parallel ice sheet model (PISM). *Journal of Glaciology*, *62*(231), 199–214. https://doi.org/10.1017/jog.2016.13